Acta Scientiarum
http://periodicos.uem.br/ojs
ISSN on-line: 1807-8664
Doi: 10.4025/actascitechnol.v47i1.70856

Spatio-temporal distribution evolution and factors controlling landslides in Beichuan County after Wenchuan earthquake

Qinghai Deng[1], Lulu Xu[1,2,3], Liping Zhang[1*], Ping Li[1], Ning Ding[1] and Qiao Chen[1]

[1]College of Earth Science and Engineering, Shandong University of Science and Technology, No.579 Qianwangang Road, Huangdao District, Qingdao City, Shandong Province, China. [2]Key Laboratory of Geological Safety of Coastal Urban Underground Space, Ministry of Natural Resources, Qingdao City, Shandong Province, China. [3]Qingdao Geologic and Mineral Geotechnical Engineering Co., Ltd, Qingdao City, Shandong Province, China. *Author for correspondence. E-mail: zhangliping@sdust.edu.cn

ABSTRACT. The earthquake triggered numerous secondary geological disasters, mainly landslides, which can have considerable impact on the environment as well as people's lives in the affected region. In this research, to obtain clear understanding of the restoration level and the evolution of landslides after an earthquake as massive as the Wenchuan earthquake, Beichuan County of Sichuan Province was considered an example, and the development characteristics and the evolution of post-earthquake landslides in the affected area were studied. Using ALOS, GF-1, and ZY-3 remote sensing images and GIS technology, the development of landslides in Beichuan County over a period of 13 years (2007–2019), comprising the period before and after the Wenchuan earthquake, was analysed. The main inducing factors of landslides before and after the disaster were discussed from many aspects. After the Wenchuan earthquake, the number and the area affected by landslides in Beichuan County drastically increased. Five years after the earthquake, there was rapid recovery in the development of landslides; however, it has not fully returned to the state before the earthquake yet. Many landslides have also occurred in medium- and high-altitude areas and medium- and high-slope areas. However, as time goes on, the high-risk areas of landslides began to migrate slowly to areas with lower altitude and gentle slope. Before the earthquake, river erosion was the main cause of landslides in the study area. After the earthquake, landslides were concentrated in the southeast and central parts of this area—places with strong earthquake intensities—which was attributed to seismogenic faults. With the recovery of landslide development, river erosion became the main contributing factor again. The findings of this research can provide insights to aid disaster prevention in the Wenchuan earthquake-stricken area and the spatio-temporal evolution of landslide disaster development in earthquake-stricken areas.

Keywords: landslide; restoration level; evolution; Beichuan County; Wenchuan earthquake

Received on Dezember 28, 2023.
Accepted on February 03, 2025.

Introduction

Earthquakes cause many landslides and affect large areas (Lu et al., 2022; Xie et al., 2022). The casualties caused by the landslides are second only to the earthquake itself. These landslides are extremely destructive to natural resources, ecosystems, and infrastructure (Aditian et al., 2018), thus exacerbating the negative social and economic impact of the earthquake (Valagussa et al., 2019). The magnitude 8.5 earthquake in Haiyuan, Ningxia Hui Autonomous Region, China in 1920 caused thousands of loess landslides, leading to thousands of deaths and river blockages (Zhuang et al., 2018). The Ludian magnitude 6.7 earthquake in 2014 induced at least 1,024 landslides that were > 100 m^2, with a total area of 5.19 km^2 (Xu et al., 2014). After the magnitude 7 earthquake in Jiuzhaigou, Sichuan Province, China in 2017, a large area of landslides ruined the roads in this scenic area, resulting in the drying up of many lakes (Wang et al., 2018). As one of the most catastrophic natural disasters in China in recent years, the Wenchuan Ms 8 earthquake on 12 May, 2008 caused a large number of secondary geological disasters (Lan & Chen, 2020; Liu et al., 2021; Yuan et al., 2022), resulting in a large number of casualties and property loss (Guo et al., 2015; Li et al., 2022; Luo et al., 2023). As the most serious secondary disaster after an earthquake, landslides have attracted the attention of many experts at home and abroad, and they have carried out various studies, such as susceptibility evaluation, landslide occurrence mechanism, risk analysis, and post-earthquake deformation (Chen et al., 2012; Deng et al., 2017; Diao et al., 2018; Fan, Zhan, et al., 2018; Huang et al., 2012; Huang & Li, 2014; Jiang et al., 2017; Li et al., 2022; Xu et al., 2014). However, most of these studies have focused on landslides occurring during

the earthquake or within a few years after the earthquake; there is scant research on the post-earthquake evolution of landslides over time. Landslide activities could last for a long time after an earthquake. Although the impact of the earthquake on landslides gradually weakens over time, the landslides in Wenchuan have not yet recovered to the state before the earthquake. Therefore, it is necessary to study the development characteristics and spatio-temporal evolution of landslides after the earthquake to aid local disaster prevention.

Yingxiu and Beichuan were the two areas that suffered the most serious damage and casualties in the 2008 Wenchuan earthquake (Dai et al., 2011; Li et al., 2023; Zhang et al., 2010). Moreover, Beichuan is located on the Longmenshan fault zone, and the rupture on the earth's surface caused by the earthquake also passed through Beichuan. Therefore, to some extent, the earthquake in Beichuan was stronger than that in the epicentre area (Yingxiu) (Zhuang et al., 2018). Taking Beichuan as an example, by comparing the development characteristics of landslides before the earthquake, this study examines the evolution of the landslides after the Wenchuan earthquake, providing insights on the recovery of landslides after the earthquake and the variation of inducing factors in this area.

A regional landslide survey usually covers a large region with complex terrain and geological conditions. This makes it challenging to understand the distribution of landslides in a short period of time via conventional survey methods (Kumar et al., 2018; Wang et al., 2023). Remote sensing detection technology was developed in the 1960s, and it has been widely used in the extraction of ground objects (Kincey et al., 2014; Di Martire et al., 2017; Prince, 2019; Smith et al., 2019; Sòria-Perpinyà et al., 2020). Remote sensing can rapidly and clearly identify the shape, tone, texture, and surrounding disaster formative environment of landslides (Feng et al., 2020; Fu, 2023; Huang et al., 2023; Zhang et al., 2021).Thus, it has become essential in the fields of landslide hazard analysis, sensitivity evaluation, identification, and emergency treatment. Using aerial photos and the digital elevation model in the north Aso volcano, Atsuhisa Yano et al. (Yano et al., 2019) studied the distribution of Aso volcanic landslides from the list of six landslides from 1955 to 2016. Darya Golovko et al. (Golovko et al., 2017) used time-series remote sensing data to reconstruct a large-scale landslide event at the foot of the Tianshan Mountain in Osh, Kyrgyzstan and analysed the likelihood and risk of landslides in this region. Wang et al. (Wang et al., 2019) used PlanetScope images to analyse landslides triggered by the Iburi Mw 6.6 earthquake in Eastern Hokkaido in 2018 and summarised the landslide distribution and the controlling factors. Taking Beichuan as an example, in this study, the landslide development characteristics of Beichuan in the 13 years before and after the Wenchuan earthquake are analysed using remote sensing images, and the impact of the Wenchuan earthquake on landslides in this area are discussed.

Material and methods

Overview of the earthquake-stricken area

Beichuan is located in Mianyang, Sichuan (Figure 1), with coordinates of 103°44′–104°42′ East longitude and 31°14′–32°14′ North latitude. Located in the northwest of the Sichuan Basin, the county is dotted with mountains and crisscrossing valleys. Beichuan stretches to the Minshan mountains in the west and Longmenshan Mountains in the east. It has a subtropical monsoon climate, i.e., the whole county is warm and humid with adequate rain. The annual average rainfall is 1,399.1 mm, and the rainy season mainly lasts from June to August. A developed river system runs through the county. There is lush vegetation with a forest coverage rate of 46.93%.

The Wenchuan earthquake occurred on 12 May, 2008 (Figure 2). It caused the dislocation of two large thrust faults in the Longmenshan thrust belt on the eastern edge of the Qinghai Tibet Plateau, forming a 240 km-long surface fracture zone along the Beichuan fault and a 72 km-long surface fracture zone along the Pengxian County–Guanxian County fault. The maximum vertical and horizontal offsets along the Beichuan fault zone are 6.5 m and 4.9 m, respectively (Xu et al., 2009). The large-scale thrust and strike-slip movement caused by the Wenchuan earthquake in the fault zone destroyed the stability of the rock bodies (Cui et al., 2011), causing a large number of collapses, landslides, and mudslides (Liu et al., 2023; Tian et al., 2023; Zhang et al., 2016). The landslides caused by the Wenchuan earthquake mainly occurred near the Beichuan–Yingxiu and Pengxian–Guanxian fault zones, especially in the upper-plate of the Beichuan–Yingxiu fault zone. The places that suffered the most include Yingxiu, Dujiangyan, Wenchuan, Beichuan, Mianyang, and Jiangyou. The upper-plate of the Beichuan–Yingxiu fault zone is mountainous, and the terrain is complex with a high degree of relief; this region was seriously affected by the landslides (Tian et al., 2023). The lower-plate of the Beichuan–Yingxiu fault zone is, however, in the low-lying Sichuan Basin, which was slightly affected by the landslides. Yuan et al. (Yuan et al., 2013) determined that > 70% of the co-seismic landslides occurred in the

southwest and middle of the Beichuan–Yingxiu fault zone; the number and frequency of landslides was also high near the main rivers. Dai et al. (Dai et al., 2011) categorised these landslide movements as shallow broken landslides, rock collapses, deep landslides, and rock avalanches. The most common ones are shallow landslides and rock collapses from steep hillsides. Deep landslides are also common, but these mostly occur near fault zones. Other types of landslides mostly occur near mountain ridges.

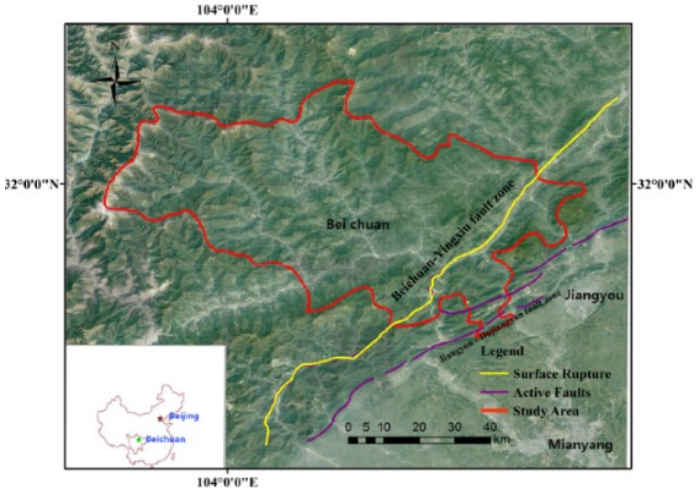

Figure 1. Overview of the earthquake-stricken area.

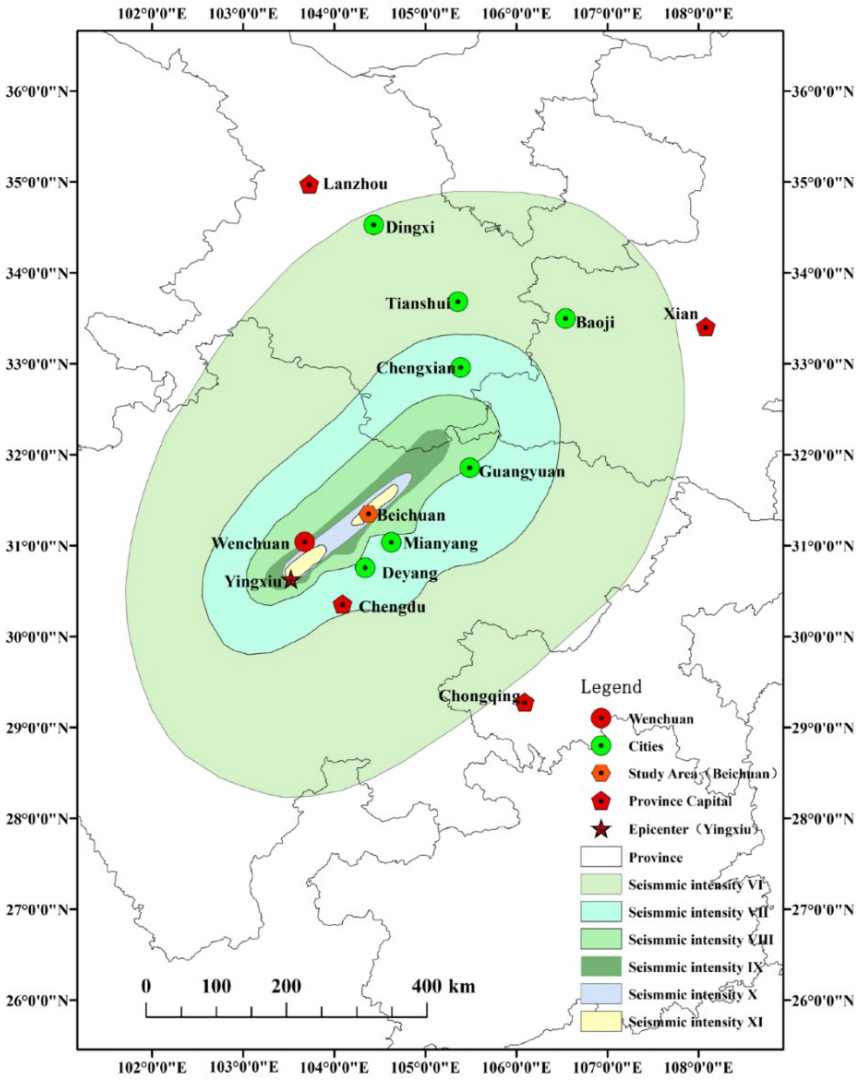

Figure 2. Intensity map of the Wenchuan earthquake.

Landslides, collapses, and mudslides triggered by the Wenchuan earthquake have caused considerable damage in the earthquake-stricken region (Wu et al., 2022; X. Zhang et al., 2022). In Beichuan, there have been new geological disasters in > 500 locations, and many villages or communities in Qushan, Leigu, and Chenjiaba have been completely buried. The towns of Xuanping and Yuli were flooded by the barrier lake. The total area of collapsed, broken, or significantly damaged buildings in the urban and rural areas was 981 million m^2 , and a total of 8,605 lives were lost. In particular, landslides in Chenjiaba Yingtaogou, Beichuan Xinzhong, Hanjiashan, Hongyan village, and Taihong village have caused > 30 casualties. The smallest disaster mass of the Hanjiashan landslide group reached 300,000 m3, while the largest one, the Chenjiaba landslide, reached 12 million m^3 (Yin, 2008). The Wangjiayan landslide in the old urban area of Beichuan led to a disaster volume of 4.8 million m^3 and caused 1,600 deaths. It was one of the most severe landslides resulting from the earthquake. Using FLAC3D simulation, Yin et al. (Yin et al., 2015) obtained the shear strain increment and the displacement contours; the Wangjiayan landslide was found to be stable before the Wenchuan earthquake, but the shear strain increment after the earthquake was approximately 3,000 times that before the main shock. Li et al. (Li et al., 2016) simulated the failure of Wangjiayan landslides and analysed the movement of the failure bodies from the aspects of displacement, velocity, effective plastic strain field, and topographic change in movement. The Tangjiashan landslide was located on the bank of Jianjiang River in Dashui village, Qushan town, Beichuan County, towards the west of the northern part of Longmenshan Mountain. It was a large-scale and hazardous secondary geological disaster induced by the Wenchuan earthquake (Li et al., 2010). The Tangjiashan barrier lake formed by the Tangjiashan landslide was the largest one formed by this earthquake, with a volume of 2.4×10^8 m^3. Six towns and two cities downstream of the landslide dam were at the risk of dam breakage and flood, posing a huge threat to a population of approximately 1.2×10^6 downstream.

Data and methods

This study used 9 ALOS, 4 ALOS, 12 ZY-3, 20 GF-1, 14 ZY-3, and Google Earth images obtained in 2007, 2010, 2013, 2015, 2017, and 2019, respectively, and ASTER GDEM data with 30 m resolution. The panchromatic resolution of the ALOS Image was 2.5 m. The ZY-3 satellite, launched in January 2012, had a panchromatic resolution of 2.1 m. The GF-1, launched in April 2013, had a panchromatic resolution of 2 m and a multispectral resolution of 8 m. The research results of Fang et al. (Fang et al., 2012) are adopted herein as the landslide data after the earthquake.

The remote sensing images of each year in the study area were obtained and corrected, registered, spliced, fused, and cropped using ENVI software. The terrain of the landslide in the study area appeared in various shapes such as armchairs and tongues and with irregular geometries. The double grooves were homologous, and the colour tone was dark. Key features, such as the landslide wall, the edge of the landslide, the steps of the landslide, and the tongue of the landslide, were clear. According to these identification marks, landslides in the study area over the years were visually interpreted (Figure 3).

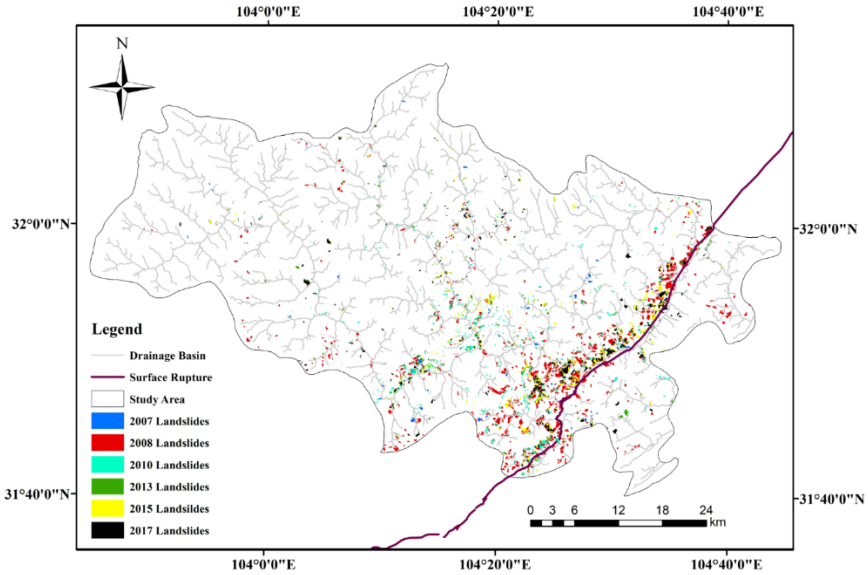

Figure 3. Distribution of landslides in Beichuan over the years.

Variations in the number of landslides, distribution area, density, and landslide plane area in Beichuan before and after the Wenchuan earthquake were analysed based on these interpretation results. The landslide distribution map was superimposed on the topographic factors (Figure's 4 and 5), the river system (Figure 6), the seismogenic fault (Figure 1), and the seismic intensity distribution map (Figure 7). The relationship and changes between these factors were analysed, revealing the evolution and development of landslides before and after the earthquake.

(Figure 4) shows the elevation reclassification thematic map of the study area; the elevations therein are divided into five levels: 500 ~ 1,000 m, 1,000 ~ 1,500 m, 1,500 ~ 2,000 m, 2,000 ~ 2,500 m, and > 2,500 m.

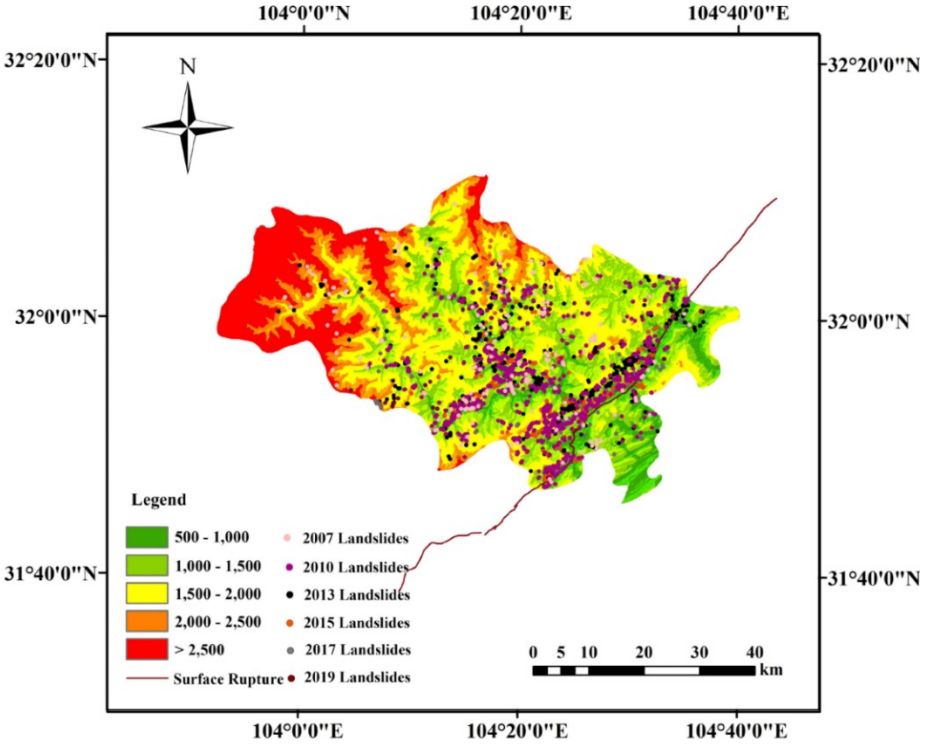

Figure 4. Elevation reclassification thematic map of Beichuan.

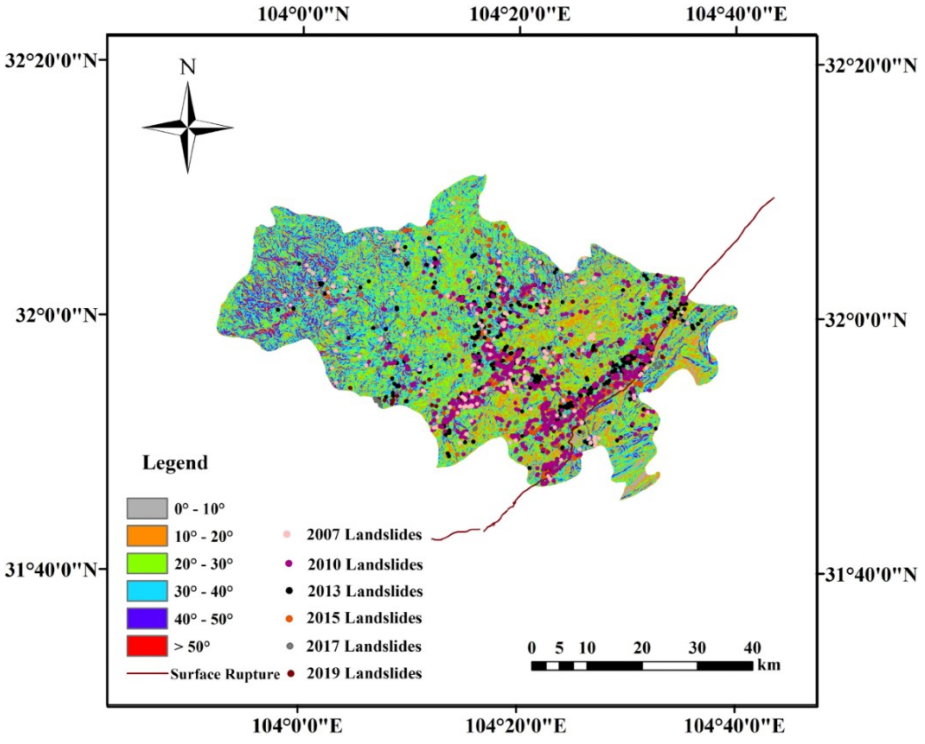

Figure 5. Slope reclassification thematic map of Beichuan.

(Figure 5) shows the slope reclassification thematic map of the study area. First, the slopes of Beichuan were extracted using the 30 m resolution DEM data and then divided into six categories: 0° ~ 10°, 10° ~ 20°, 20° ~ 30°, 30° ~ 40°, 40° ~ 50°, and > 50°.

(Figure 6) shows the distribution map of the river system buffer zones in the study area. The zones are established in a sequence of 200 m, 400 m, 600 m, 800 m, 1000 m, and 1,200 m, with the river system as the centre.

The seismic intensity distribution map of the study area adopts an intensity distribution map of the Wenchuan earth-quake (China Earthquake Administration, 2008) compiled by the China Geological Survey (Figure 7). The seismic inten-sity in Beichuan can be divided into four grades; it gradually decreases as the distance from the seismogenic fault zone increases, and the area of the upper wall of the seismogenic fault with the highest intensity is larger than that of the lower wall.

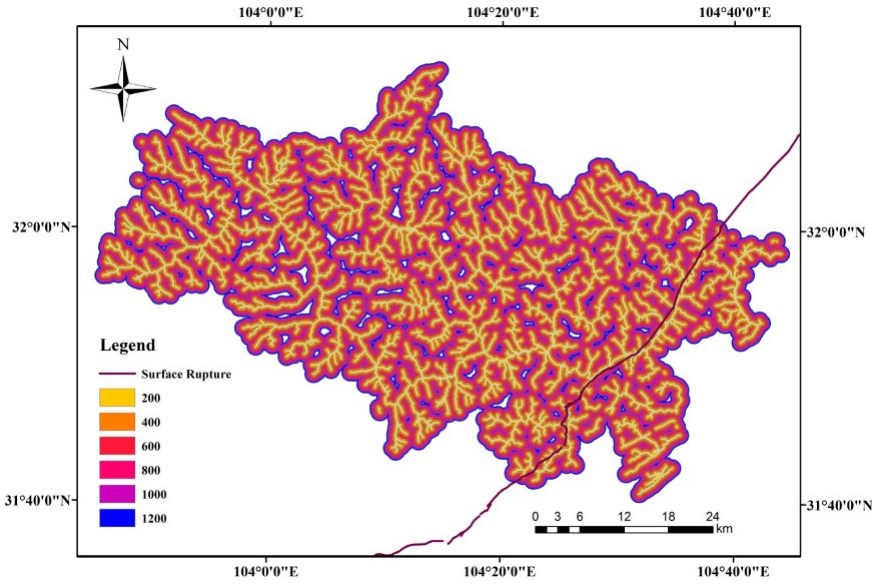

Figure 6. Distribution map of the river system buffer zones.

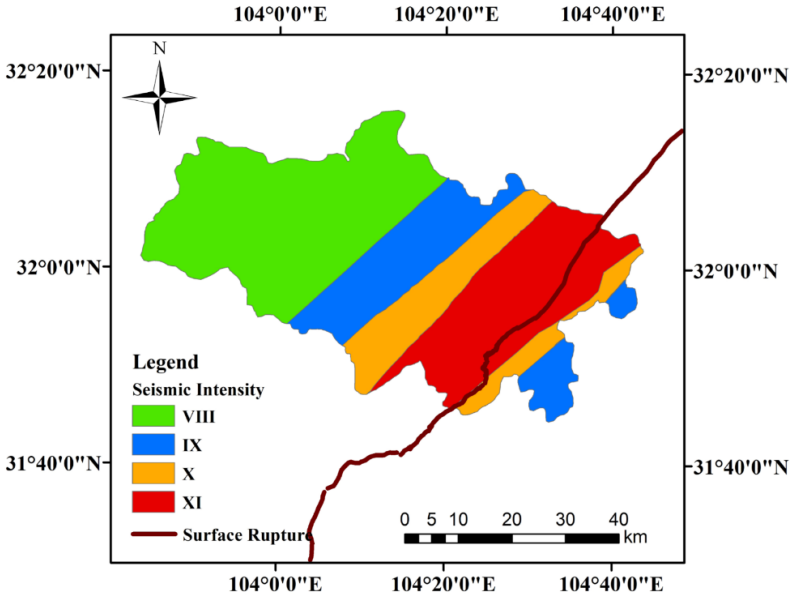

Figure 7. Seismic intensity distribution map of Beichuan during the Wenchuan earthquake.

Results

Change in number of landslides and distribution area

Before the Wenchuan earthquake in 2008, frequent landslides did not occur in Beichuan. In 2007, 200 landslides were interpreted in the whole county, with a distribution area of only 5.07 km^2. Due to the

Wenchuan earthquake, Beichuan has become one of the most severely impacted places, and it has also led to many landslides, resulting in a sharp increase in the number and distribution area of the disasters (distribution area of landslides > 50 km^2, estimated total volume of landslides > 25×10^6 m^3) (Fan, Scaringi, et al., 2018; Fang et al., 2012). In 2010, 937 landslides were interpreted that were distributed across an area of 14.59 km^2. Specifically, certain rainstorms also led to severe consequences. For example, during the '8-13', '8-19', and '9-09' floods in 2010, the number of disasters increased considerably. Compared with 2010, the number of landslides decreased by 29.67% in 2013; the total distribution area of landslides, however, increased to 14.77 km^2. This was also mainly attributed to rainstorms. For example, from 8 to 12 July, 2013, there was a rainstorm in the Beichuan region, and it caused a large number of geological disasters. On 16 July, 2013, Chenjiaba of Guixi counties witnessed sudden mudslides triggered by the rainstorm. More than 500,000 m^3 of mud and rocks rushed into the Qinglin gully, raising the riverbed by nearly 4 m, forming a barrier lake (Li & She, 2015; Tang & Wang, 2015; Wang et al., 2014). Within five years after the earthquake, because of the ruptured surface of the earth, loose rock and soil mass, and frequent rainstorms, the recovery of landslide in Beichuan was not significant. In 2015, the total number of landslides in Beichuan decreased to 475, with a distribution area of 14.44 km^2 (decrease of 27.92% compared to 2013); this shows that landslides in this area began to enter a relatively stable recovery period. In 2017, the total number of landslides decreased to 358 (decrease of 24.63% compared with 2015), and the distribution area decreased to 10.19 km^2. By 2017, nine years after the earthquake, although the development of landslides in Beichuan had not recovered to the level before the earthquake, there has been significant progress in landslide recovery; compared with 2010, the number of landslides had decreased by 60% and the distribution area of landslides had decreased by 30%. By 2019, the total number of landslides had decreased to 315, with a total area of 8.42 km^2, showing slight landslide recovery compared with 2017.

Change in landslide density

Landslide density was calculated as the relative index for earthquake intensity using the core density calculation tool in ArcGIS. Based on landslide density, the earthquake activity intensity of the regional geological disasters was divided into three levels, i.e., areas with landslide density < 0.1 km^{-2}, 0.1–1 km^{-2}, and > 1 km^{-2} were less developed areas, moderately developed areas, and more developed areas, respectively. (Figure 8) shows the density variation of landslides in Beichuan before and after the Wenchuan earthquake. Before the Wenchuan earthquake, the landslide activity in this area was weak; only some sporadically distributed small areas were identified as more developed areas, and the distribution of moderately developed areas was relatively uniform. The distribution of landslide disasters in the study area before the earthquake is not largely influenced by seismic structures. After the Wenchuan earthquake, the more developed areas expanded, especially in the first few years after the earthquake, and strong landslide development areas increased sharply. Landslides were concentrated in the centre and southeast of this area and were influenced by seismic structures. Specifically, the southeast of the study area, located near the Longmenshan surface fracture zone, suffered the most damage from severe landslides. Over time, landslides in the central area gradually decreased. Landslide distribution area in the southeast was decreasing, but it was still the main affected area, indicating that the impact of the Wenchuan earthquake on the slope would not disappear soon enough. Table 1 shows the annual proportion of different landslide development areas. (Figure 9) shows the annual change in different types of development areas. According to Table 1 and (Figure 9), the area with strong landslide development before the disaster (2007) was very small, accounting for only 0.4% of the whole county; the whole county mainly comprised less developed areas. A few years after the earthquake (2008–2010), many less developed areas swiftly transformed into medium or strong landslide development areas. After 2010, these areas slowly increased, and after 2013, they started increasing considerably and gradually approached the level before the earthquake. The size of the moderately developed area showed an increasing trend from 2008 to 2013, and then, after peaking in 2013, it decreased every year. The size of the more developed area peaked in 2010 and then began to decrease every year, indicating that the impact of the Wenchuan earthquake on landslide development in this area gradually weakened since 2010. From 2010 to 2013, the increase in the less developed area was insignificant, and the moderately developed area reached its peak in 2013. This was mainly attributed to the frequent rainstorms in the study area during this period, which influenced the restoration of landslides to some extent. After 2015, the growth of the less developed area tended to stabilise, indicating that the recovery process had entered a stage with reduced recovery speed. By 2019, 11 years after the earthquake, although the impact of the earthquake had gradually weakened,

landslide development had not fully returned to the level before the earthquake. It is a long process for the landslides in Beichuan to return to the state before the 2008 Wenchuan Ms 8 earthquake.

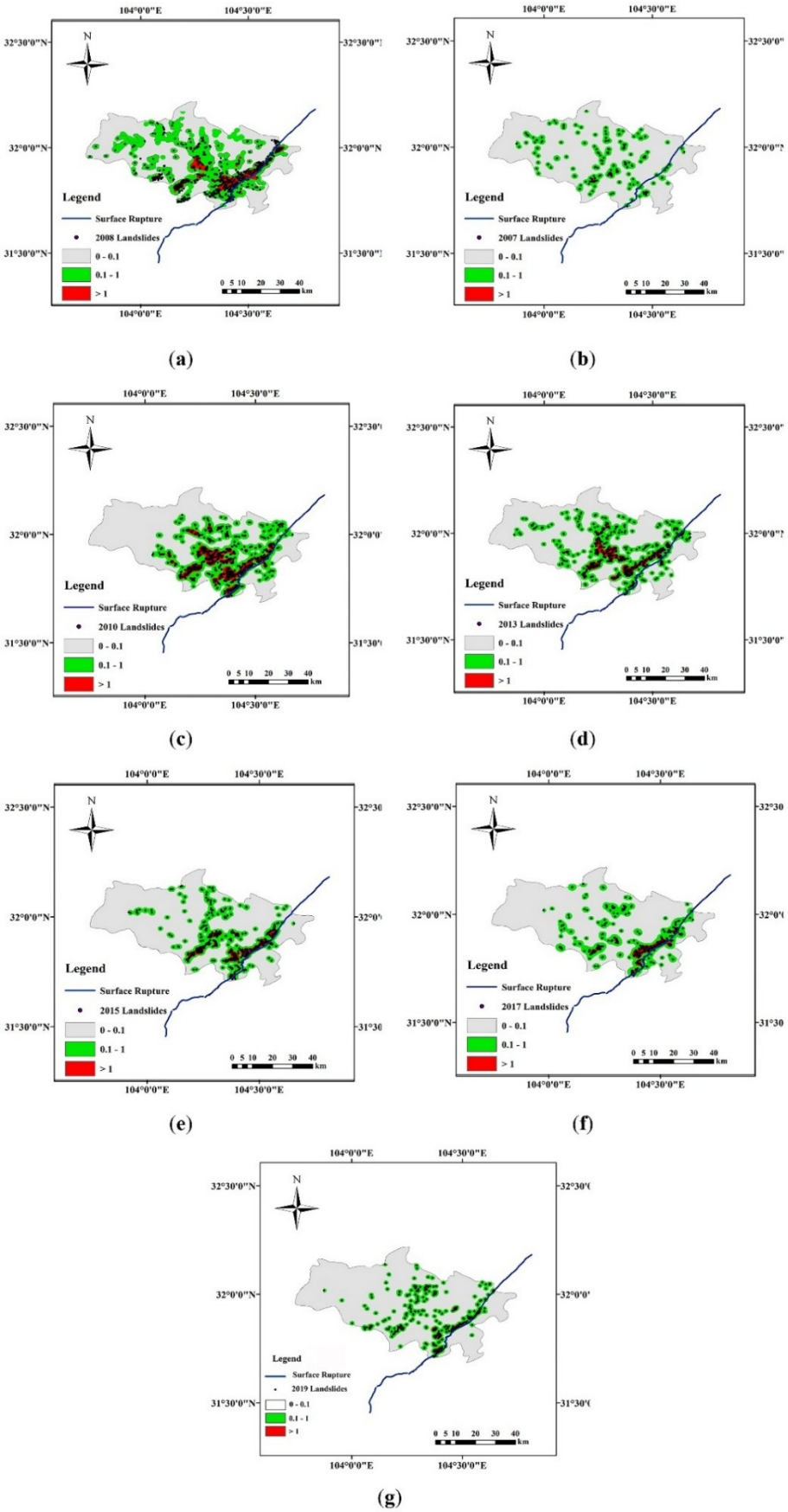

Figure 8. Annual landslide density distribution; (a) 2007, (b) 2008, (c) 2010, (d) 2013, (e) 2015, (f) 2017, (g) 2019.

Table 1. Classification of landslide development.

	2007	2008	2010	2013	2015	2017	2019
Less developed area	80.03%	62.5%	58.84%	61.39%	73.32%	74.56%	79.78%
Moderately developed area	19.57%	30%	30.07%	32.32%.	21.88%	22.41%	17.74%
More developed area	0.4%	7.5%	11.09%	6.29%	4.80%	3.03%	2.48%

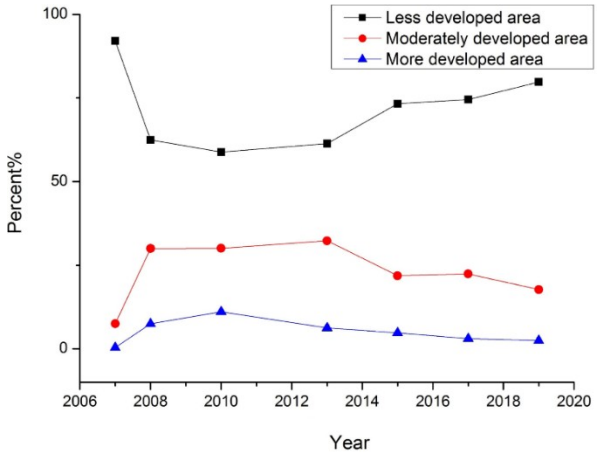

Figure 9. Landslide density variation with time in different development areas.

Changes in landslide area

According to the area, the landslides can be divided into **six** categories, namely, 0–0.01, 0.01–0.025, 0.025–0.05, 0.05–0.075, 0.75–0.1, and > 0.1 (km^2) (Li et al., 2018). (Figure 10) shows the annual distribution of the number of landslides in different areas. Before the earthquake, landslides in the study area were mainly in the range of 0–0.01 km^2, followed by 0.01–0.025 km^2 and 0.025–0.05 km^2, and landslides in other sizes were uncommon. In contrast, after the earthquake, the number of landslides in the range of 0–0.01 km^2 was still the highest every year, especially in 2010. Heavy rainfalls in that year caused local landslides, with more landslides with smaller areas. Landslides with areas of 0.01–0.025 km^2 and 0.025–0.05 km^2 also increased significantly and showed a decreasing trend every year after 2013. In 2013, although the number of small-scale landslides decreased significantly, the number of medium-sized landslides increased compared to that in 2010 because of the extreme rainfalls in 2012 and 2013. Although there were fewer landslides with sizes of 0.075–0.1 km^2 and > 0.1 km^2, their numbers decreased significantly slowly than among other categories. In particular, the number of landslides with size of > 0.1 km^2 stabilised during the first couple of years after the earthquake. Before 2015, the number of 0–0.01 km^2 landslides decreased rapidly, while that of 0.01–0.025 km^2, 0.025–0.05 km^2, and 0.05–0.075 km^2 decreased slowly. After 2015, the number of 0–0.01 km^2 landslides decreased slowly. By 2017, the number of 0.05–0.075 km^2 landslides decreased significantly, along with 0.75–0.1 km^2 and > 0.1 km^2 landslides, indicating that the number of medium and large landslides decreased gradually. By 2019, the number of 0.75–0.1 km^2 and > 0.1 km^2 landslides changed only slightly, suggesting that the recovery of larger landslides takes some time.

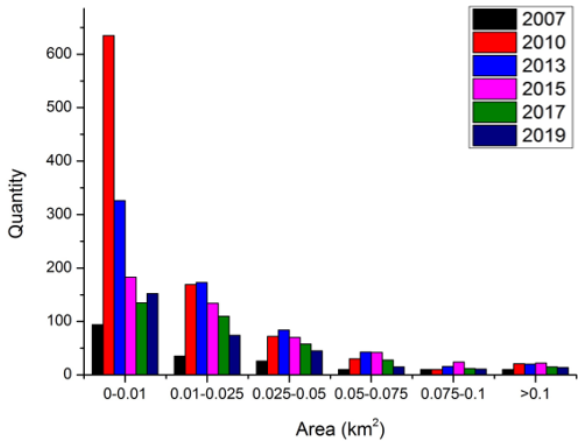

Figure 10. Number of landslides of different areas in each year.

Relationship between landslides and topographic factors

Relationship between landslides and elevation

The landslide distribution of each year was superimposed with the elevation data to obtain the landslide distribution of each year within different elevation ranges (Figure 11). Before the earthquake, 92.63% of the landslides occurred on slopes with elevation < 2,000 m, 43.81% occurred in the elevation range of 500–1,000 m, 33.53% occurred in the range of 1,000–1,500 m, 15.29% occurred in the range of 1,500–2,000 m, and only a small number of landslides occurred > 2,000 m. According to Fang et al. (Fang et al., 2012), after the 2008 earthquake, most landslides still occurred below the elevation range of 2,000 m, and the proportion increased, accounting for 95.4%. In particular, 56.9% landslides occurred in the elevation range of 1,000–2,000 m, and 38.5% occurred < 1,000 m, both of which show significantly increases compared to that before the earthquake. From 2008 to slightly before 2017, most landslides occurred within the elevation range of 1,000–1,500 m. By 2017, most landslides occurred in the elevation of 500–1,000 m. By 2019, the number of landslides within the elevation range of 500m-1000m decreased slightly, but its proportion was higher than that in 2017, indicating that the more developed areas have gradually shifted to low altitude areas. (Figure 4) shows that the area above 2,000 m was mainly located in the west of the study area. In addition to the factor of high altitude, the area was also far away from the seismogenic fault zone and less affected by the earthquake; therefore, there were fewer landslides. In comparison, the altitude in the east of the study area was < 2,000 m and close to the seismogenic fault zone. Consequently, there were many landslides in this area before the earthquake, which primarily occurred at the foot of the mountain (elevation < 1,000 m). After the earthquake, the number and ratio of landslides within the elevation range of 1,000–2,000 m increased, suggesting that the earthquake destroyed the stability of the ridge and the slope near the mountain top. Since 2013, the number of landslides in the elevation ranges of 1,000–1,500 m and 1,500–2,000 m started decreasing. This shows that through the action of internal and external forces over the years, the landslides progressed towards areas with lower elevations. The number of landslides in the region with elevation > 2,500 m remained unchanged before and after the earthquake. Compared to before the earthquake, there were more landslides in the elevation range of 2,000–2,500 m after the earthquake, but the number was relatively stable.

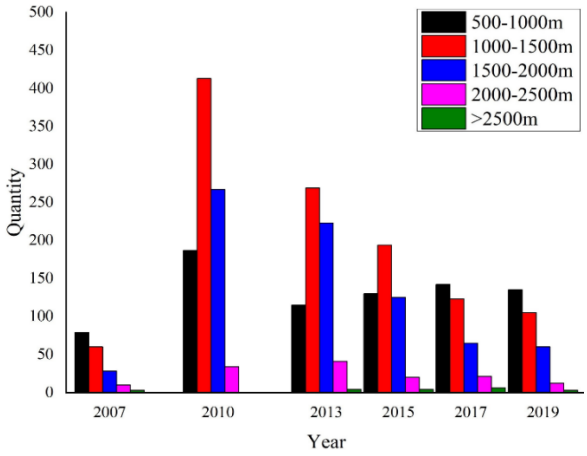

Figure 11. Bar chart of landslide distribution with elevation.

Relationship between landslide and slope

Figure 12 shows the relationship between the landslide and slope for different years. Before and after the earthquake, most landslides occurred on 20°–50° slopes. Before the earthquake, only a few landslides occurred in areas with slope > 50°; after the earthquake, the number of such landslides increased. Over time, the number of these landslides decreased, and by 2017, this number had decreased to the level before the earthquake. From the Wenchuan earthquake in 2008 to 2010, the number of landslides on 20°–50° slopes increased and then decreased after 2010. The number of landslides on slopes of other degrees decreased after 2008, indicating that the recovery speeds of landslides on flat and steep slopes were faster. After several heavy rainfalls in 2013, the number of landslides in the 30°–40° slopes decreased, while the proportion of landslides in the 10°–30° slope increased. This indicated that some debris on steep slopes gradually migrated to the flatter slopes because of the rainfall, increasing the probability of landslides. From the point of level of

recovery, areas with steep slopes were less affected by the external force factors, so the recovery was the best. Among other slopes, the recoveries of areas with slope = 10°–20° and 20°–25° were relatively good. Compared with that before the earthquake, the number of landslides in areas with slope = 0°–10° changed only slightly. By 2019, the number of landslides had recovered to that before the earthquake. In areas with small slopes, landslides do not occur easily; therefore, there were fewer landslides in this area. For areas that are most prone to landslides, the degree of recovery was also relatively high (Chen et al., 2021).

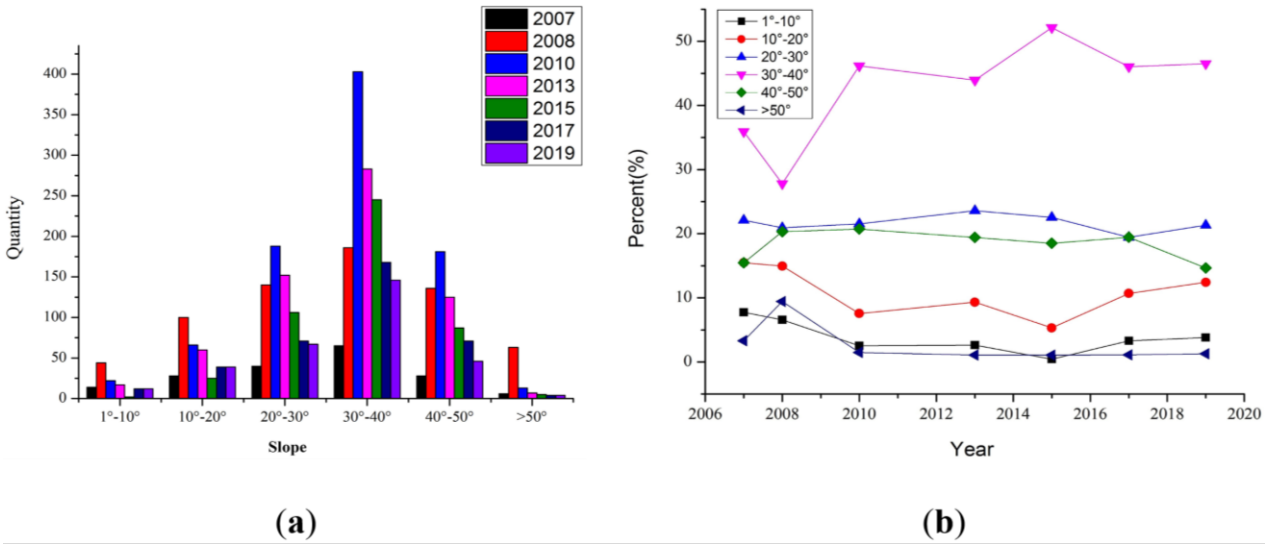

Figure 12. Relationship between number of landslides and slopes in different years; (a) bar chart; (b) variation of the number of landslides with time for different slope ranges.

Relationship between landslide and river system

The river system buffer zone map was overlapped with that of distribution of landslides to obtain the distribution of landslides with the river system distance (Figure 13). Before as well as after the earthquake, probability of landslides occurring was higher closer to the river system. Before the earthquake, many landslides occurred in the area 0–200 m away from the river system, accounting for > 50% of the total. After the earthquake, there were still many landslides in that range, but the number was significantly smaller. The number of landslides within 0–200 m away from the river system decreased in 2010 and 2013 and then increased, indicating that river erosion was not the main factor affecting occurrence of landslides in 2010 or 2013. In 2017, the number of landslides within 0–200 m away from the river system was > 50%, which was similar to that before the earthquake, indicating that the river system has once again become the main influencing factors.

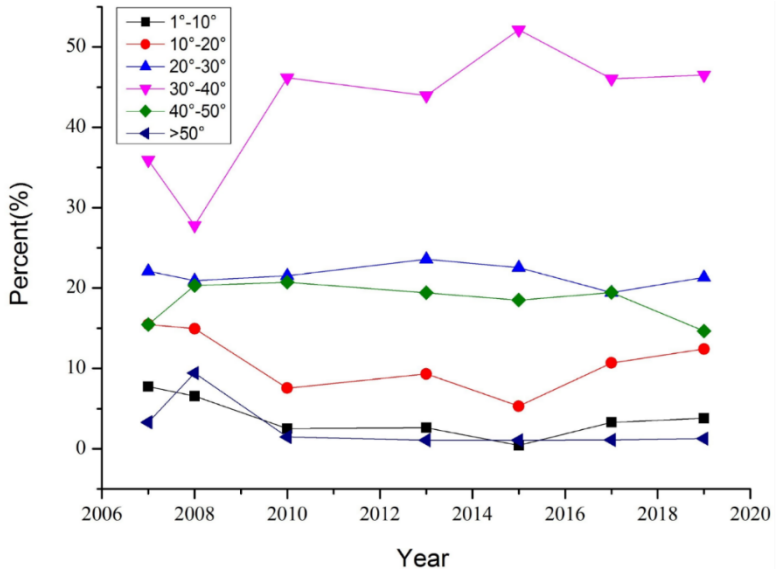

Figure 13. Distribution of landslides with the river system.

The number of landslides in all river system buffer zones peaked in 2010 and decrease thereafter every year. Compared with 2008, buffer zones with the largest increase in 2010 were 400–600 m and 600–800 m away from the river system. Compared with 2010, the number of landslides within 400–600 m and 600–800 m away from the river system showed a significant decrease in 2019, suggesting that the landslides in these two areas recovered relatively well but had not yet reached the level before the earthquake.

Relationship between landslides and seismogenic faults

The Beichuan–Yingxiu fault zone was the main seismogenic fault zone of the Wenchuan earthquake. (Figure 14) shows the number of landslides within different distances from the fault. Before the earthquake, the landslide density within 2–4 km away from the seismogenic fault zone was the highest, followed by that within 2 km and 10 km away. The relationship between the distribution of landslides in this period and the seismogenic fault zone was not very clear, indicating that fault activity was not the main factor affecting the distribution of the landslides. After the earthquake, the activity of the fault zone significantly aggravated the landslide activity, i.e., landslide density was higher closer to the fault zone. In 2010 and 2013, the density distribution of the landslide sites changed due to heavy rainfalls, and the landslide density in areas far from the fault zone increased. (Figure 8) also shows that the area with serious landslides after the earthquake was towards the centre and southeast of the study area, which is close to the seismogenic fault zone. Over time, the area with serious landslides in the centre of the study area decreased after a short expansion; only a small area remained by 2017, and it further decreased by 2019. For the area close to the fault zone in the southeast of the study area, however by 2019, there were fewer but serious landslides.

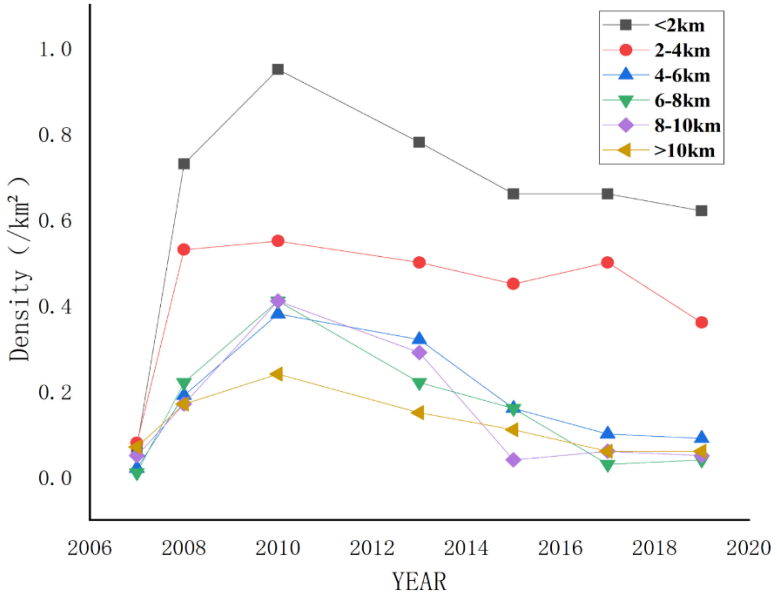

Figure 14. Variation of landslide density with fault distance in different years.

Relationship between landslide and earthquake intensity

Figure 15 shows the distribution of the number of landslides in areas with different earthquake intensities in different years. Before the earthquake, the distribution of landslides in each category was relatively even, and the one with the largest number fell in the category intensity XI. After the earthquake, the number of landslides was proportional to the earthquake intensity. In 2008, there was no significant change in the number of landslides in the area with intensity VIII. The number of landslides in the area with seismic intensities IX and X increased, and the area with the strongest seismic intensity, XI, experienced the largest increase. In the first ten years since the earthquake, the number of landslides in the area with intensity VIII was relatively stable, remaining almost unchanged compared with that before the earthquake, and it decreased from 2015 to less than that before the earthquake. In areas with intensities IX, X, and XI, the number of landslides increased since the earthquake and then decreased after 2013. The number of landslides in areas with earthquake intensities IX and X decreased sharply, reaching the levels before the earthquake by 2017; thereafter, there was no significant reduction by 2019. For the area with earthquake intensity XI, the number of landslides decreased slightly, but it remained an area with severe landslides.

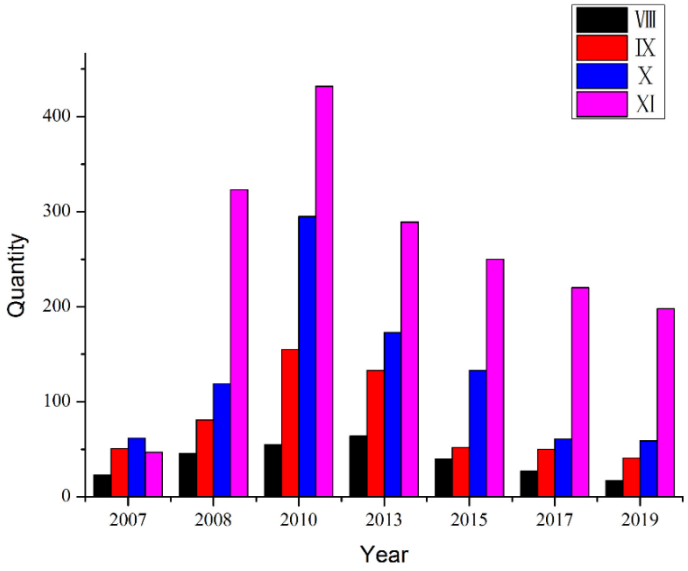

Figure 15. Bar chart distribution of landslide number and seismic intensity.

Discussion

According to the characteristics of landslide development in Beichuan before and after the earthquake, landslide development in the study area can be divided into five stages. Before the earthquake, landslide development was evenly distributed in the study area along the river; it was stable and not intense, which is called the normal development period before the earthquake. From 2008 to 2010, the occurrence of the earthquake directly impacted the distribution of landslides; the number and area of landslides increased considerably, and the area of frequent landslides expanded, suggesting that the development of landslides entered the earthquake-induced stage. From 2010 to 2013, due to aftershocks, rainfalls after the earthquake, and other factors, the number and area of landslides further expanded and more areas were affected by the landslides, indicating that the development of landslides entered the post-earthquake development stage. From 2013 to 2017, the number and area of landslides, as well as the affected area, began to decrease significantly, and thereafter, the development of landslides entered a rapid recovery stage. After 2017, the decrease in the number and area of landslides decelerated, and the development of landslides entered a stable recovery stage.

The earthquake reduced the strength of rocks and generated a lot of slope cracks, making it easier for rainwater to penetrate the rocky slopes. Rainfall considerably influences slope stability and landslide behaviour after an earthquake (Chen et al., 2019; Yang et al., 2019). Once rainwater has penetrated the rock slope, it can change the mechanical properties of the rock and the soil by reducing their strengths, while the infiltrated rainwater can add to the weight of the rock and soil, creating a seepage force and increasing the landslide sliding force, thus increasing the probability of landslides (Chen & Zhang, 2014). Under the combined influence of the earthquake and rainfall, landslide activities were relatively strong in Beichuan in the first five years after the earthquake. In particular, the '8-13' and '8-19' floods in 2010, the '8-17' floods in 2012, and a 300-mm rainfall in 2013 (the heaviest in 50 years) further exacerbated the landslides. During this period, rainfall dominated the distribution of landslides to some extent. After 2013, the development of landslides in the study area started to recover steadily. By 2019, the number of landslides had decreased significantly, and the area affected by landslides had gradually decreased, entering a stable recovery stage where the impact of the earthquake had decreased (Xiong et al., 2022).

Before the earthquake, the landslides were more influenced by river erosion than other factors; more distance from the river implied less susceptibility to landslides. After the earthquake, the number of landslides in other areas increased, but it was highest close to the river, suggesting that the impact of the earthquake was superimposed on the regional background conditions.

Areas with gentle slopes and low altitudes are prone to landslides due to frequent human activities (McAdoo et al., 2018). Therefore, the post-disaster reconstruction work is also mainly concentrated in these areas, such as the construction of small towns, houses, roads, and even small hydropower stations. These constructions not only influence the stability of nearby rock slopes, but also produce a large number of artificial ones, increasing the probability of landslides.

The restoration of landslides is also closely related to the vegetation. In high-altitude areas, vegetation restoration is limited by environmental conditions. Therefore, although landslides are relatively less likely to happen in high-altitude areas, the restoration is also relatively slow. Furthermore, at high altitudes, sunny slopes recover better than shady ones (Gorokhovich & Vustianiuk, 2021). Sunny slopes experience considerable environmental changes and strong evaporation, which reduces soil water content and makes soil loose; however, they also have a suitable environment for vegetation growth. Vegetation therefore recovers faster and better after the disaster, contributing to the satisfactory recovery of landslides. The growth of vegetation also closely depends on soil nutrients. The accumulation of soil organic matters in the landslide area is slow and fertiliser retention is poor, because of which vegetation restoration is difficult. In areas with steep slopes, soil nutrients may be lost to areas with lesser slopes due to rainfall erosion, making this area suitable for accumulation of nutrients and providing a good environment for growth of vegetation (Chen et al., 2022). Therefore, landslide recovery is better in areas with smaller slopes.

Areas struck by strong earthquakes are prone to landslides for long durations, especially exacerbated by rainfall, weathering, and erosion. Landslides in the study area were not very active before the strong 2008 earthquake. Although more landslides are likely to happen in the area closer to the fault zone, there was no obvious difference in the actual occurrences of landslides. After the Wenchuan earthquake, the number of landslides increased considerably, being inversely proportional to the distance from the fault zone, and the frequency of landslides also decreased significantly. More importantly, the relationship between the number of landslides and the distance of the seismogenic fault zone became obvious (Qin et al., 2023). By 2017, the area closest to the seismogenic fault zone was still the main landslide area. As of 2019, although the number of landslides in this area had decreased, their scales increased under the influence of extreme climate. Therefore, under the combined influence of the earthquake, climate, and other factors, landslides in this area are expected to remain active for a long time. Extreme rainfall may induce large-scale landslides and rush the deposits to places with lower elevations and gentler slopes (Wang et al., 2023).

Conclusion

When the earthquake happened, The landslides activities were influenced by the seismogenic fault. After the earthquake, The main factor affecting landslide shifts has shifted from rivers to fault zones. But the distribution of the water system remained the main role.

Within the first few years after the earthquake, landslides in this area began to recover. Nine years later, landslide recovery had improved. In the meantime, the number of landslides in high slope and high altitude increased. Specifically, small- and medium-sized landslides have recovered to a higher level than the large ones.

Acknowledgments

The authors acknowledge the support and facilities provided by the Computer Network Information Center, Chinese Academy of Sciences. Mean while, a special thanks are given to Researcher Yuan Renmao of Institute of Geology, China Seismological Bureau for his guid-ance on this work. At the same time, we thank the editors and reviewers for their valuable comments.

References

Aditian, A., Kubota, T., & Shinohara, Y. (2018). Comparison of GIS-based landslide susceptibility models using frequency ratio, logistic regression, and artificial neural network in a tertiary region of Ambon, Indonesia. *Geomorphology, 318*, 101–111. https://doi.org/10.1016/j.geomorph.2018.06.006

Chen, H. X., & Zhang, L. M. (2014). A physically-based distributed cell model for predicting regional rainfall-induced shallow slope failures. *Engineering Geology, 176*, 79–92. https://doi.org/10.1016/j.enggeo.2014.04.011

Chen, M., Tang, C., Li, M., Xiong, J., Luo, Y., Shi, Q., Zhang, X., Tie, Y., & Feng, Q. (2022). Changes of surface recovery at coseismic landslides and their driving factors in the Wenchuan earthquake-affected area. *CATENA, 210*, 105871. https://doi.org/10.1016/j.catena.2021.105871

Chen, M., Tang, C., Wang, X., Xiong, J., Shi, Q., Zhang, X., Li, M., Luo, Y., Tie, Y., & Feng, Q. (2021). Temporal and spatial differentiation in the surface recovery of post-seismic landslides in Wenchuan

earthquake-affected areas. *Ecological Informatics, 64*, 101356. https://doi.org/10.1016/j.ecoinf.2021.101356

Chen, X. L., Ran, H. L., & Yang, W. T. (2012). Evaluation of factors controlling large earthquake-induced landslides by the Wenchuan earthquake. *Natural Hazards and Earth System Sciences, 12* (12), 3645–3657. https://doi.org/10.5194/nhess-12-3645-2012

Chen, Y., Irfan, M., Uchimura, T., Wu, Y., & Yu, F. (2019). Development of elastic wave velocity threshold for rainfall-induced landslide prediction and early warning. *Landslides, 16* (5), 955–968. https://doi.org/10.1007/s10346-019-01138-2

Cui, P., Chen, X.-Q., Zhu, Y.-Y., Su, F.-H., Wei, F.-Q., Han, Y.-S., Liu, H.-J., & Zhuang, J.-Q. (2011). The Wenchuan Earthquake (May 12, 2008), Sichuan Province, China, and resulting geohazards. *Natural Hazards, 56* (1), 19–36. https://doi.org/10.1007/s11069-009-9392-1

Dai, F. C., Xu, C., Yao, X., Xu, L., Tu, X. B., & Gong, Q. M. (2011). Spatial distribution of landslides triggered by the 2008 Ms 8.0 Wenchuan earthquake, China. *Journal of Asian Earth Sciences, 40* (4), 883–895. https://doi.org/10.1016/j.jseaes.2010.04.010

Deng, Q., Gong, L., Zhang, L., Yuan, R., Xue, Y., Geng, X., & Hu, S. (2017). Simulating dynamic processes and hypermobility mechanisms of the Wenjiagou rock avalanche triggered by the 2008 Wenchuan earthquake using discrete element modelling. *Bulletin of Engineering Geology and the Environment, 76* (3), 923–936. https://doi.org/10.1007/s10064-016-0914-2

Di Martire, D., Paci, M., Confuorto, P., Costabile, S., Guastaferro, F., Verta, A., & Calcaterra, D. (2017). A nation-wide system for landslide mapping and risk management in Italy: The second Not-ordinary Plan of Environmental Remote Sensing. *International Journal of Applied Earth Observation and Geoinformation, 63*, 143–157. https://doi.org/10.1016/j.jag.2017.07.018

Diao, F., Wang, R., Wang, Y., Xiong, X., & Walter, T. R. (2018). Fault behavior and lower crustal rheology inferred from the first seven years of postseismic GPS data after the 2008 Wenchuan earthquake. *Earth and Planetary Science Letters, 495*, 202–212. https://doi.org/10.1016/j.epsl.2018.05.020

Fan, X., Scaringi, G., Xu, Q., Zhan, W., Dai, L., Li, Y., Pei, X., Yang, Q., & Huang, R. (2018). Coseismic landslides triggered by the 8th August 2017 Ms 7.0 Jiuzhaigou earthquake (Sichuan, China): Factors controlling their spatial distribution and implications for the seismogenic blind fault identification. *Landslides, 15* (5), 967–983. https://doi.org/10.1007/s10346-018-0960-x

Fan, X., Zhan, W., Dong, X., Van Westen, C., Xu, Q., Dai, L., Yang, Q., Huang, R., & Havenith, H.-B. (2018). Analyzing successive landslide dam formation by different triggering mechanisms: The case of the Tangjiawan landslide, Sichuan, China. *Engineering Geology, 243*, 128–144. https://doi.org/10.1016/j.enggeo.2018.06.016

Fang, D., Hu, Z. W., & Wang, Z. H. (2012). Spatial prediction of earthquake secondary landslide disaster in Beichuan County based on GIS. *Journal of Mountain, 30* (2), 230–238.

Feng, W. K., Dun, J. W., Yi, X. Y., & Zhang, G. Q. (2020). Deformation analysis of Woda Village giant landslide in Jinsha River Basin based on SBAS-InSAR technology. *Journal of Engineering Geology, 28* (2), 384–393. https://doi.org/10.13544/j.cnki.jeg.2019-411

Fu, G. X. (2023). Resurrection characteristics and risk assessment of coseismic landslide based on InSAR technology. *Southwest University of Science and Technology*.

Golovko, D., Roessner, S., Behling, R., Wetzel, H.-U., & Kleinschmit, B. (2017). Evaluation of remote-sensing-based landslide inventories for hazard assessment in Southern Kyrgyzstan. *Remote Sensing, 9* (9), 943. https://doi.org/10.3390/rs9090943

Gorokhovich, Y., & Vustianiuk, A. (2021). Implications of slope aspect for landslide risk assessment: A case study of Hurricane Maria in Puerto Rico in 2017. *Geomorphology, 391*, 107874. https://doi.org/10.1016/j.geomorph.2021.107874

Guo, D. P., He, C., Xu, C., & Hamada, M. (2015). Analysis of the relations between slope failure distribution and seismic ground motion during the 2008 Wenchuan earthquake. *Soil Dynamics and Earthquake Engineering, 72*, 99–107. https://doi.org/10.1016/j.soildyn.2015.02.001

Huang, F., Xiong, H., Yao, C., Catani, F., Zhou, C., & Huang, J. (2023). Uncertainties of landslide susceptibility prediction considering different landslide types. *Journal of Rock Mechanics and Geotechnical Engineering*. https://doi.org/10.1016/j.jrmge.2023.03.001

Huang, R., & Li, W. (2014). Post-earthquake landsliding and long-term impacts in the Wenchuan earthquake area, China. *Engineering Geology, 182*, 111–120. https://doi.org/10.1016/j.enggeo.2014.07.008

Huang, R., Pei, X., Fan, X., Zhang, W., Li, S., & Li, B. (2012). The characteristics and failure mechanism of the largest landslide triggered by the Wenchuan earthquake, May 12, 2008, China. *Landslides, 9* (1), 131–142. https://doi.org/10.1007/s10346-011-0276-6

Jiang, Z., Yuan, L., Huang, D., Yang, Z., & Chen, W. (2017). Postseismic deformation associated with the 2008 Mw 7.9 Wenchuan earthquake, China: Constraining fault geometry and investigating a detailed spatial distribution of afterslip. *Journal of Geodynamics, 112*, 12–21. https://doi.org/10.1016/j.jog.2017.09.001

Kincey, M., Batty, L., Chapman, H., Gearey, B., Ainsworth, S., & Challis, K. (2014). Assessing the changing condition of industrial archaeological remains on Alston Moor, UK, using multisensor remote sensing. *Journal of Archaeological Science, 45*, 36–51. https://doi.org/10.1016/j.jas.2014.02.008

Kumar, V., Gupta, V., & Jamir, I. (2018). Hazard evaluation of progressive Pawari landslide zone, Satluj valley, Himachal Pradesh, India. *Natural Hazards, 93* (2), 1029–1047. https://doi.org/10.1007/s11069-018-3339-3

Lan, J., & Chen, X. L. (2020). Evolution characteristics of landslides triggered by 2008 Ms8.0 Wenchuan earthquake in Yingxiu area. *Seismology and Geology, 42* (1), 125–146.

Li, C. R., Wang, M., & Liu, K. (2018). A decadal evolution of landslides and debris flows after the Wenchuan earthquake. *Geomorphology, 323*, 1–12. https://doi.org/10.1016/j.geomorph.2018.09.010

Li, F., Zhai, P., Huang, J., & Tan, H. (2022). Influences of the heterogeneity of viscoelastic medium on postseismic deformation of the 2008 MW7.9 Wenchuan earthquake. *Geodesy and Geodynamics, 13* (1), 1–10. https://doi.org/10.1016/j.geog.2021.08.006

Li, M. W., Xiong, J., Chen, M., & Tang, C. (2023). Vegetation restoration and dynamic evolution of coseismic landslide activity in Wenchuan earthquake area. *Hydrogeological Engineering Geology, 50* (3), 182–192. https://doi.org/10.16030/j.cnki.issn.1000-3665.202209049

Li, P. P., & She, T. (2015). Distribution characteristics of geological hazards induced by heavy rainfall in Beichuan County. *Science and Technology Outlook, 25* (26), 172.

Li, S. D., Li, X., Zhang, J., He, J. M., Li, S. H., & Wang, Y. C. (2010). Study on the genetic mechanism of Tangjiashan landslide and the overall stability of dam. *Journal of Rock Mechanics and Engineering, 29* (S1), 2908–2915.

Li, X., Wu, Y., He, S., & Su, L. (2016). Application of the material point method to simulate the post-failure runout processes of the Wangjiayan landslide. *Engineering Geology, 212*, 1–9. https://doi.org/10.1016/j.enggeo.2016.07.014

Liu, B., Hu, X. W., & He, K. (2023). Study on the distribution characteristics and disaster model of earthquake cracks in Wenchuan strong earthquake area. *Disaster Science*, 1–15.

Liu, Z. J., Tan, K., Wang, Q., Wang, L., Zhang, J., Zhao, B., & Qiao, X. J. (2021). Numerical simulation analysis of post-seismic afterslip and viscoelastic relaxation following the Wenchuan earthquake. *Geodesy and Geodynamics, 41* (6), 577–583. https://doi.org/10.14075/j.jgg.2021.06.005

Lu, J., Li, W., Zhan, W., & Tie, Y. (2022). Distribution and mobility of coseismic landslides triggered by the 2018 Hokkaido earthquake in Japan. *Remote Sensing, 14* (16), 3957. https://doi.org/10.3390/rs14163957

Luo, G., Chen, X., Zhang, Q., He, K., Wu, M., Shen, W., & Liu, B. (2023). Failure mechanism and sedimentary characteristics of a catastrophic rockslide avalanche induced by the 2008 Wenchuan earthquake. *Landslides, 20* (1), 25–38. https://doi.org/10.1007/s10346-022-01955-y

McAdoo, B. G., Quak, M., Gnyawali, K. R., Adhikari, B. R., Devkota, S., Rajbhandari, P. L., & Sudmeier-Rieux, K. (2018). Roads and landslides in Nepal: How development affects environmental risk. *Natural Hazards and Earth System Sciences, 18* (12), 3203–3210. https://doi.org/10.5194/nhess-18-3203-2018

Prince, S. D. (2019). Challenges for remote sensing of the Sustainable Development Goal SDG 15.3.1 productivity indicator. *Remote Sensing of Environment, 234*, 111428. https://doi.org/10.1016/j.rse.2019.111428

Qin, Y., Zhang, D., Zheng, W., Yang, J., Chen, G., Duan, L., Liang, S., & Peng, H. (2023). Interaction of earthquake-triggered landslides and local relief: Evidence from the 2008 Wenchuan earthquake. *Landslides, 20* (4), 757–770. https://doi.org/10.1007/s10346-022-01996-3

Smith, W. K., Dannenberg, M. P., Yan, D., Herrmann, S., Barnes, M. L., Barron-Gafford, G. A., Biederman, J. A., Ferrenberg, S., Fox, A. M., Hudson, A., Knowles, J. F., MacBean, N., Moore, D. J. P., Nagler, P. L., Reed, S. C., Rutherford, W. A., Scott, R. L., Wang, X., & Yang, J. (2019). Remote sensing of dryland ecosystem structure and function: Progress, challenges, and opportunities. *Remote Sensing of Environment, 233*, 111401. https://doi.org/10.1016/j.rse.2019.111401

Sòria-Perpinyà, X., Vicente, E., Urrego, P., Pereira-Sandoval, M., Ruíz-Verdú, A., Delegido, J., Soria, J. M., & Moreno, J. (2020). Remote sensing of cyanobacterial blooms in a hypertrophic lagoon (Albufera of València, Eastern Iberian Peninsula) using multitemporal Sentinel-2 images. *Science of The Total Environment, 698*, 134305. https://doi.org/10.1016/j.scitotenv.2019.134305

Tang, J. F., & Wang, Q. (2015). Analysis of geological disasters in Beichuan settlement space in 2013. *Disaster Science, 30* (1), 87–91.

Tian, Y., Huang, H., Xie, Z. S., She, T., & Li, J. Y. (2023). History and formation mechanism of Tangjiawan landslide in Beichuan segment of Yingxiu-Beichuan fault zone. *Sedimentation and Tethyan Geology, 43* (3), 629–639. https://doi.org/10.19826/j.cnki.1009-3850.2022.03004

Valagussa, A., Marc, O., Frattini, P., & Crosta, G. B. (2019). Seismic and geological controls on earthquake-induced landslide size. *Earth and Planetary Science Letters, 506*, 268–281. https://doi.org/10.1016/j.epsl.2018.11.005

Wang, F., Fan, X., Yunus, A. P., Siva Subramanian, S., Alonso-Rodriguez, A., Dai, L., Xu, Q., & Huang, R. (2019). Coseismic landslides triggered by the 2018 Hokkaido, Japan (Mw 6.6), earthquake: Spatial distribution, controlling factors, and possible failure mechanism. *Landslides, 16* (8), 1551–1566. https://doi.org/10.1007/s10346-019-01187-7

Wang, J., Jin, W., Cui, Y., Zhang, W., Wu, C., & Alessandro, P. (2018). Earthquake-triggered landslides affecting a UNESCO Natural Site: The 2017 Jiuzhaigou Earthquake in the World National Park, China. *Journal of Mountain Science, 15* (7), 1412–1428. https://doi.org/10.1007/s11629-018-4823-7

Wang, S. Y., Ye, T. L., Lu, X. B., & Nie, X. Y. (2014). Numerical simulation of Beichuan slope failure under rainfall conditions. *Chinese Journal of Geological Hazards and Prevention, 25* (2), 43–48. https://doi.org/10.16031/j.cnki.issn.1003-8035.2014.02.011

Wang, X., Zhang, S., Zhang, H., Wang, D., Bai, M., Li, W., Li, S., Sun, T., & Wang, Y. (2023). Prediction of landslide susceptibility in Wenchuan County based on pixel-level samples. *Bulletin of Engineering Geology and the Environment, 82* (6), 203. https://doi.org/10.1007/s10064-023-03230-3

Wu, X. Y., Xu, C., Xu, X. W., Chen, G. H., Zhu, A. L., Zhang, L., Yu, G., & Du, K. (2022). A Web-GIS hazards information system of the 2008 Wenchuan Earthquake in China. *Natural Hazards Research, 2* (3), 210–217. https://doi.org/10.1016/j.nhres.2022.03.003

Xie, J., Coulthard, T. J., Wang, M., & Wu, J. (2022). Tracing seismic landslide-derived sediment dynamics in response to climate change. *CATENA, 217*, 106495. https://doi.org/10.1016/j.catena.2022.106495

Xiong, J., Tang, C., Tang, H., Chen, M., Zhang, X., Shi, Q., Chang, M., Gong, L., Li, N., & Li, M. (2022). Long-term hillslope erosion and landslide–channel coupling in the area of the catastrophic Wenchuan earthquake. *Engineering Geology, 305*, 106727. https://doi.org/10.1016/j.enggeo.2022.106727

Xu, C., Xu, X., Yao, X., & Dai, F. (2014). Three (nearly) complete inventories of landslides triggered by the May 12, 2008 Wenchuan Mw 7.9 earthquake of China and their spatial distribution statistical analysis. *Landslides, 11* (3), 441–461. https://doi.org/10.1007/s10346-013-0404-6

Xu, X., Wen, X., Yu, G., Chen, G., Klinger, Y., Hubbard, J., & Shaw, J. (2009). Coseismic reverse- and oblique-slip surface faulting generated by the 2008 Mw 7.9 Wenchuan earthquake, China. *Geology, 37* (6), 515–518. https://doi.org/10.1130/G25462A.1

Yang, Z., Cai, H., Shao, W., Huang, D., Uchimura, T., Lei, X., Tian, H., & Qiao, J. (2019). Clarifying the hydrological mechanisms and thresholds for rainfall-induced landslide: In situ monitoring of big data to unsaturated slope stability analysis. *Bulletin of Engineering Geology and the Environment, 78* (4), 2139–2150. https://doi.org/10.1007/s10064-018-1295-5

Yano, A., Shinohara, Y., Tsunetaka, H., Mizuno, H., & Kubota, T. (2019). Distribution of landslides caused by heavy rainfall events and an earthquake in northern Aso Volcano, Japan from 1955 to 2016. *Geomorphology, 327*, 533–541. https://doi.org/10.1016/j.geomorph.2018.11.024

Yin, Y., Li, B., & Wang, W. (2015). Dynamic analysis of the stabilized Wangjiayan landslide in the Wenchuan Ms 8.0 earthquake and aftershocks. *Landslides, 12* (3), 537–547. https://doi.org/10.1007/s10346-014-0497-6

Yin, Y. P. (2008). A study on geological disasters caused by Wenchuan M = 8 earthquake. *Journal of Engineering Geology, 04*, 433–444.

Yuan, R.-M., Deng, Q.-H., Cunningham, D., Xu, C., Xu, X.-W., & Chang, C.-P. (2013). Density distribution of landslides triggered by the 2008 Wenchuan earthquake and their relationships to peak ground acceleration. *Bulletin of the Seismological Society of America, 103* (4), 2344–2355. https://doi.org/10.1785/0120110233

Yuan, X., Liu, C., Nie, R. H., Yang, Z. L., Li, W. L., Dai, X. A., Cheng, J. Y., Zhang, J. M., Ma, L., Fu, X., Tang, M., Xu, Y. N., & Lu, H. (2022). A comparative analysis of certainty factor-based machine learning methods for collapse and landslide susceptibility mapping in Wenchuan County, China. *Remote Sensing, 14* (14), 3259. https://doi.org/10.3390/rs14143259

Zhang, P.-Z., Wen, X., Shen, Z.-K., & Chen, J. (2010). Oblique, high-angle, listric-reverse faulting and associated development of strain: The Wenchuan earthquake of May 12, 2008, Sichuan, China. *Annual Review of Earth and Planetary Sciences, 38* (1), 353–382. https://doi.org/10.1146/annurev-earth-040809-152602

Zhang, X., Tang, C., Li, N., Xiong, J., Chen, M., Li, M., & Tang, C. (2022). Investigation of the 2019 Wenchuan County debris flow disaster suggests nonuniform spatial and temporal post-seismic debris flow evolution patterns. *Landslides, 19* (8), 1935–1956. https://doi.org/10.1007/s10346-022-01896-6

Zhang, Y. S., Guo, C. B., Yao, X., Yang, Z. H., Wu, R. A., & Du, G. L. (2016). A study on geological hazard effects of active faults on eastern margin of Qinghai-Tibet Plateau. *Acta Geographica Sinica, 37* (03), 277–286.

Zhang, Y. S., Liu, X. Y., Wu, R. A., Guo, C. B., & Ren, S. S. (2021). Ancient landslide in deep valley area on eastern edge of Qinghai-Tibet Plateau: Identification, characteristics, age and evolution. *Earth Science Frontiers, 28* (02), 94–105. https://doi.org/10.13745/j.esf.sf.2020.9.10

Zhuang, J., Peng, J., Xu, C., Li, Z., Densmore, A., Milledge, D., Iqbal, J., & Cui, Y. (2018). Distribution and characteristics of loess landslides triggered by the 1920 Haiyuan Earthquake, Northwest of China. *Geomorphology, 314*, 1–12. https://doi.org/10.1016/j.geomorph.2018.04.012